

- [13] a) C. Tschierske, *J. Mater. Chem.* **1998**, *8*, 1485. b) C. M. Paleos, D. Tsiourvas, *Angew. Chem. Int. Ed. Engl.* **1995**, *34*, 1696.
- [14] a) G. A. Jeffrey, *Acc. Chem. Res.* **1986**, *19*, 168. b) G. A. Jeffrey, L. M. Wingert, *Liq. Cryst.* **1992**, *12*, 179.
- [15] a) H. A. van Doren, L. M. Wingert, *Recl. Trav. Chim. Pays-Bas* **1994**, *113*, 260. b) J. W. Goodby, G. H. Mehl, I. M. Saez, R. P. Tuffin, G. Mackenzie, R. Auzély-Velty, T. Benvegnu, D. Plusquellec, *Chem. Commun.* **1998**, 2057.
- [16] 2,3,6,7,10,11-Hexakis(1-carboxypentyl-6-oxy)triphenylene and 2,3,6,7,10,11-hexakis(1-carboxydecyl-6-oxy)triphenylene were obtained by coupling the benzyl ester protected 6-bromohexanoic acid and 11-bromoundecanoic acid, respectively, with 2,3,6,7,10,11-hexahydroxytriphenylene (N. Boden, R. C. Borner, R. J. Bushby, A. N. Cammidge, M. V. Jesudason, *Liq. Cryst.* **1993**, *15*, 851) and then removing the benzyl ester protecting groups by hydrogenolysis.
- [17] P. R. Ashton, C. L. Brown, S. E. Boyd, N. Jayaraman, S. A. Nepogodiev, J. F. Stoddart, *Chem. Eur. J.* **1996**, *2*, 1115.
- [18] P. R. Ashton, S. R. L. Everitt, M. Gómez-López, N. Jayaraman, J. F. Stoddart, *Tetrahedron Lett.* **1997**, *38*, 5691.
- [19] Assuming the disc-like molecules have a cylindrical shape, the molecular volume, V_{mol} is given by $\pi r^2 h$ where r is the radius of the cylinder and h is the stacking distance (parameter c) measured by X-ray diffraction. The molar volumes, V_m , in cm^3 of the compounds can be obtained by dividing their molar masses by their densities. From V_m , the molecular volume (V_{mol}) in \AA^3 can be calculated from $V_m \times 10^{24}/N_A$ where N_A is Avogadro's number.
- [20] R. Seghrouchni, A. Skoulios, *J. Phys. II Fr.* **1995**, *5*, 1385.
- [21] The following abbreviations are used: DCC = 1,3-dicyclohexylcarbodiimide, HOBT = 1-hydroxybenzotriazole, HOAT = 1-hydroxy-7-azabenzotriazole.

Thin Films of Macroporous Metal Oxides**

By Mary E. Turner, Timothy J. Trentler, and Vicki L. Colvin*

Porous solids created from colloidal crystal templates are of great interest because they can potentially offer three dimensional photonic band gaps at visible and near-infrared wavelengths.^[1,2] In these structures, ~70 % of the sample is air arranged in a hexagonal array of spherical voids. Due to the highly ordered structure, these porous solids exhibit intense optical diffraction. If diffraction from the host solid is strong enough, as would be the case for samples with indices of about 2.8,^[3] then the systems are predicted to possess a full, three-dimensional photonic bandgap. Such materials have been proposed as the centerpiece for numerous optical technologies ranging from low threshold lasers^[4] to planar waveguides.^[5] The promise of these systems has motivated a number of efforts to create ordered voids within materials, such as titanium dioxide, which offer a high refractive index with minimal absorption at visible wavelengths.^[6-22] Typically, monolithic and polycrystalline colloidal crystals, or opals, provide a removable template for structuring porous ceramics. The strong photonic properties of the resulting samples are apparent in the reflection spectra of small domains (<0.6 mm) of material.^[20-23] Here, we describe a method that produces these valuable materials as planar thin films better suited for

optical characterization and application. This format requires material strategies distinct from those employed in the templating of monolithic opals, and produces high-quality optical materials over large areas with photonic bandwidths in excess of 18 %.

To form macroporous optical films, we start by using an opal solid which is different from monoliths formed by gravity or centrifugal sedimentation. These templates consist of multilayers of close-packed colloids that are cast onto optical substrates using a convective assembly, or dip-coat process. The resulting colloidal samples are not perfect crystals, but they have no apparent grain boundaries and are effectively single crystals.^[24] Like opal minerals formed through natural sedimentation, these samples possess a periodic dielectric structure in three dimensions as well as sub-micrometer feature sizes. However, their format is more reminiscent of lithographically prepared photonic crystals in that they are relatively thin and supported by a thick underlying substrate.

Such a template geometry presents a challenge for any subsequent chemistry used to deposit solids in the crystal interstices. Prior efforts to template oxide materials into opals relied on the hydrolysis of neat metal alkoxides soaked into the pores of the structure.^[11,12,19,20] Although this procedure works well for monolithic samples, when applied to thin films it deposits an inhomogeneous layer on their surfaces that produces severe light scattering. In contrast, films of high optical quality resulted when we adapted an alternative hydrolytic method originally developed to form uniform coats of material on isolated colloids in solution.^[25] For this approach, metal alkoxides are dissolved in anhydrous alcohols and near stoichiometric quantities of water are added. The subsequent formation of hydrous oxides does not occur homogeneously throughout the solution, but rather preferentially at silica surfaces via heterogeneous nucleation. Thus, smooth and controlled oxide layers can be built up deep within the template. The resulting TiO_2 films are optically clear and uniformly colored after reaction and removal of the silica spheres (Fig. 1). We have adapted this chemistry to forming other metal ox-

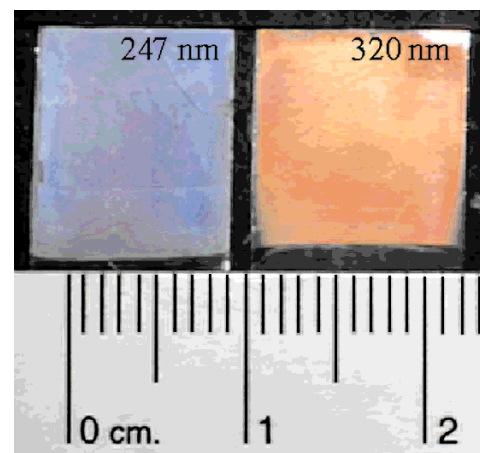


Fig. 1. Photograph of macroporous TiO_2 on PAMA backing. Pore size is 247 nm for the sample on the left (blue) and 320 nm for the sample on the right (red). The samples were illuminated with white light at normal incidence.

[*] Prof. V. L. Colvin, M. E. Turner, Dr. T. J. Trentler
Department of Chemistry
Rice University
Houston, TX 77005 (USA)
E-mail: colvin@rice.edu

[**] We thank Dr. Kristen Kulinowski, Dr. Daniel Mittleman, and Peng Jiang for many useful discussions and Bruce Brinson for assistance with characterization. This work was supported by the R. A. Welch foundation (C-1342), the Texas Advanced Technology program (Project # 003604-050), and the National Science Foundation (CHE-9704020).

ides, such as ZrO_2 and SnO_2 , but these are not emphasized here because they have lower refractive indices than titania.

As formed the hydrous titanium dioxide has a relatively low density and thus low refractive index.^[26,27] High-temperature treatments allow the material to densify and achieve a higher refractive index.^[28] To ensure that high temperatures could be accessed, a quartz substrate was used to support the silica colloidal crystal.^[29,30] These materials permitted the silica–titania composites to be stable up to 1025 °C with no degradation of their diffractive properties. During this process, both the silica and titania materials densify significantly as they lose physisorbed and/or chemisorbed water.^[28,29] Apparently, the shrinkage of the two materials is comparable as the overall shrinkage is not enough to fracture the film significantly. This is in contrast to the severe cracking observed in monolithic opal templates prepared from polystyrene colloids and titania.^[11]

One consequence of the high temperature treatments is the crystallization of the initially amorphous titania.^[25] Typically, titania crystallizes in the anatase structure and then converts to rutile at higher temperatures. Rutile is the preferred phase for photonic applications since it possesses a higher refractive index ($n \sim 2.9$) than the anatase form ($n \sim 2.5$).^[31] According to the literature, the anatase–rutile conversion can occur over a wide temperature range of 400–1200 °C (typically 600–800 °C for alkoxide derived titania) depending on the impurities that are present.^[32,33] Thermal processing up to 1050 °C, however, yielded only anatase for these samples. Zhang et al.^[34] have reported that rutile nucleates at surfaces or interfaces, so the silica may be acting in some way to inhibit this transformation.

After thermal treatments, the thin film silica–titania composites are chemically etched to remove the silica template leaving a fully porous material. For these planar formats the process can be quite disruptive to the fragile films, and can cause them to fracture into small shards. We solved this problem by using a poly(allylmethacrylate) backing to support the thin macroporous film (Fig. 2). The entire structure could then be submerged in HF to remove the microscope slides and the silica spheres. The resulting structure consisted of a thin layer of macroporous TiO_2 adhered to a solid polymer support. In addition to providing an anchor for the macroporous TiO_2 , the polymer backing facilitates handling of the samples. Other polymers could be used as a backing support as long as they have little or no optical absorption at the wavelengths of interest.

Scanning electron microscopy (SEM) images of the macroporous samples (Fig. 2) show that our method results in the formation of a highly ordered macroporous structure. Figure 2a shows a low magnification image of a region of the sample so that the overall format can be visualized. The top surface of the TiO_2 structure is very smooth over hundreds of micrometers, which reduces scattering from the surface of the crystal and allows significant optical transmission through the sample. A cross-sectional image (Fig. 2b) shows ordering of the voids perpendicular to the substrate. Typical film thickness is 3 μm and it can be tuned between 1 and 15 μm . To

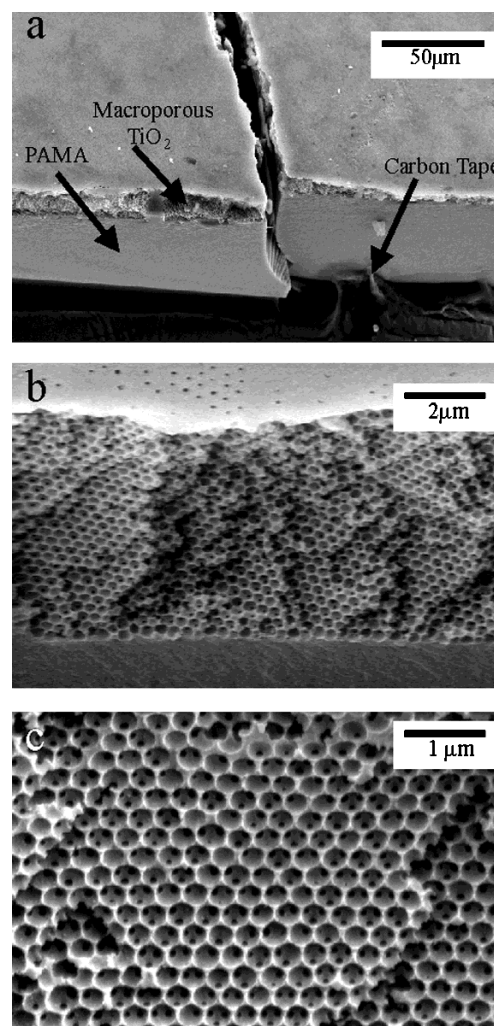


Fig. 2. SEM images of macroporous titania prepared with 351 nm diameter silica spheres. After annealing to 800 °C (4 h) spheres shrunk to 320 nm. a) Cross section of oxide with PAMA backing. The top surface of the oxide layer is smooth, allowing high-quality optical measurements. b) Cross section of the film. The small holes at the film surface are from points where the original colloids attached to the quartz substrate. c) Top-down view of pores. The top surface has been removed to reveal pores that are interconnected and close packed.

visualize the porous structure of the material, the surface layers can be removed to reveal the voids (Fig. 2c). Small ~ 70 nm holes are apparent inside the air spheres where “necks” between the original silica spheres existed. While the local ordering of the samples is evident from these images, longer range order (cm^2) is also present due to the quality of the starting template materials.^[24]

The format of our samples allows us to characterize the optical properties of these samples using transmission along the well-defined high symmetry (111) axis that is perpendicular to the underlying support material. We first verified that the optical properties of the samples behave as expected from simple considerations of diffraction from ordered dielectrics. Figure 1 shows that the photonic peak we observe is sensitive to void diameter. Additionally, our method of film deposition allows for control over sample thickness. The peak optical

density increases with increasing sample thickness (number of repeating layers), as expected (Fig. 3).^[35] Using multiple coating cycles, our technique allows for the production of samples in excess of 13 μm , or ~ 40 layers, thus even larger photonic

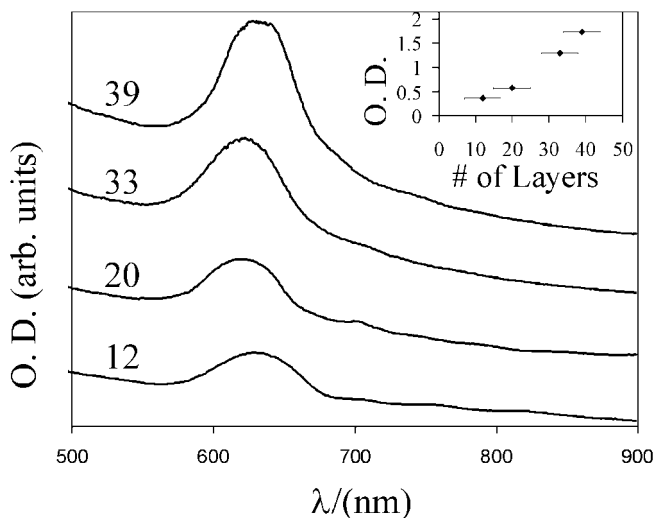


Fig. 3. Transmission spectra (90°) of macroporous titania on PAMA having thicknesses of 12, 20, 33, 39 layers. Pores are ~ 320 nm in diameter. Spectra have been offset for clarity but no background has been subtracted. The peak optical density scales well with increasing thickness of the samples, but peaks are slightly shifted due to small variations in the diameter of the air spheres. Inset: Plot of the number of layers of air spheres vs. the optical density of the stop band peak.

peaks are possible. More importantly, we found that as we increased sample thickness the peak widths stayed relatively constant once the critical thickness was achieved.^[36] Certain crystallographic defects such as dislocations or vacancies would lead to broader bandwidths, and the uniformity of this parameter with increasing thickness suggests that defects are not dominating the optical behavior.

One outstanding issue with all strategies designed to produce macroporous, high-index ceramics is the real refractive index of the interstitial material. Because the material that comprises the solid matrix is polycrystalline, it is unlikely that its refractive index is equal to that of a single crystal, bulk material.^[26] A good approximation is to assume that the optical refractive index of the ceramic material will scale proportionally with the physical density of the solid.^[27] Thus, the actual refractive index of these templated oxides will likely be lower than the numbers reported for single crystals. Since thermal treatments are known to densify ceramics, this problem may be minimized by exposing porous samples to higher temperature treatments.

Such densification does apparently occur in titania samples that are subjected to higher temperature conditions (800°C and 1025°C). Figure 4 shows that the temperature treatment led to a significant red-shift of the primary photonic peak as would be expected for a denser titania matrix. However, X-ray diffraction grain size analysis indicates that most of the crystallite grain growth is completed by 800°C with an average grain size of 20 ± 5 nm. This suggests that

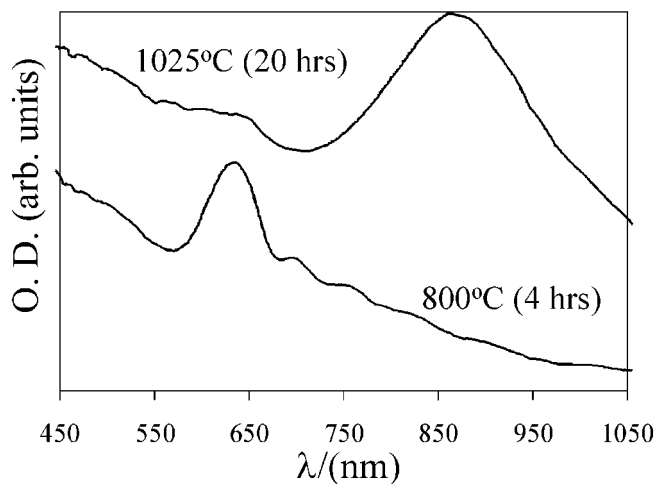


Fig. 4. Transmission spectra (90°) of macroporous titania after two different heat treatments. No background has been subtracted. The original silica sphere diameter before heating was 351 nm. In both cases the resulting air sphere diameter was ~ 320 nm. Spectra have been offset for clarity. a) 800°C for 4 h. b) 1025°C for 20 h.

between 800°C and 1025°C the titania is not densifying by grain growth, but rather by the consolidation of nanoscale pores and the removal of internal hydroxyl species. Samples treated at higher temperatures also exhibit much larger photonic bandwidths. The peak width, $\Delta\omega/\omega$, of a photonic system provides a good measure of the “strength” of a photonic band and is expected to widen as the refractive index of an inverted opal structure is increased.^[3] The data shown in Figure 4 demonstrates an increased fractional bandwidth from 7.59 % to 18.42 % in samples exposed to higher temperature thermal treatments. These bandwidths are somewhat larger than those reported in previous work on macroporous titania (12–15 %) formed from polystyrene templates.^[11,20–22] These organic colloids limit the temperature that the filled opal structures can withstand to 450 – 500°C , as opposed to the 1025°C treatments used to densify the silica–titania composites presented here.

It is difficult to obtain a quantitative value of the macroporous titania refractive index without relying on an involved theory which treats the full three-dimensional nature of the photonic band, as well as the unusual geometry of the pores. However, it is possible to estimate the refractive index for TiO_2 using a simple scalar wave approximation for hexagonal arrays of voids. From the peak positions we estimate that the refractive index of the titania increases from 1.65 (800°C) to 2.85 (1025°C).^[37] Though consistent with the expected densification of titania after higher temperature thermal treatments, this increase is clearly overestimated. The inaccuracy of this approximation is not surprising since these thermal treatments also lead to the formation of wider “necks” between adjacent silica colloids.^[30] Materials fired at 1025°C had windows between voids of ~ 140 nm diameter, while the 800°C materials possessed windows of only ~ 70 nm. Theoretical calculations have indicated that both the diameters of these interconnecting windows and the refractive index can

influence the photonic widths in porous materials.^[3] How these properties can be optimized experimentally to produce more complete photonic gaps in macroporous titania will be the subject of future work.

In summary, we have presented a strategy for making thin film macroporous oxides of large area. Since the pores are highly ordered, they possess strong diffractive properties of value in many optical applications. Such films are reminiscent in geometry to two dimensional photonic bandgap materials formed lithographically, and can be optically characterized using transmission. The focus of this work was on the generation of materials with visible optical properties, and thus with void sizes above 200 nm. It is possible to make silica sphere templates with diameters below 50 nm, and the methods reported here should extend to the formation of uniform mesoporous films.^[10]

Experimental

Colloidal Crystal Growth: Quartz microscope slides (0.5 × 2 in) are wiped with ethanol and immersed in a vial containing 15 mL of a 1 wt.-% solution of monodispersed Stober silica spheres (300, 351 nm) that are synthesized using standard methods [38]. The colloidal solution is purified by repeated centrifugation–redispersion cycles followed by dilution to the correct volume fraction. The vial is placed under a crystallizing dish to minimize airflow and contaminants. The ethanol is allowed to evaporate undisturbed at room temperature over several days resulting in a planar, close-packed crystal with few defects [24]. Approximately 200 spheres on each resulting film are analyzed using SEM (Philips XL30 SEM/FEG) to determine size and size distribution.

Thicker crystals can be formed by coating another film of spheres onto an existing film. The first film is dried for several hours prior to dipping it into a solution of the same size of nanospheres and allowing the ethanol to evaporate. The resulting films are heated in air in a muffle furnace (4 °C/min, 300 °C, 3 h to strengthen the sample and connect the spheres.

Titania Coating: The crystalline film adhered to the quartz slide is then immersed in 50 mL of anhydrous ethanol (200 proof Pharmco) under N₂. A small amount of deionized water (288 μL) is injected and mixed thoroughly with the ethanol. Then, 136 μL of titanium(IV) ethoxide (Aldrich) is added to the solution with vigorous stirring. The resulting solution is refluxed under a continuous flow of N₂ for 8 h without stirring. Within approximately 10 min the solution turns cloudy due to TiO₂ particle formation. The crystalline film coated slide is then sintered in a muffle furnace at 600 °C (4 °C/min) for 1 h after which the temperature is increased to 800 °C (3 °C/min) for 4 h or to 1025 °C (3 °C/min) for 20 h. Significant shrinkage of the silica spheres and the TiO₂ coating occurs during this heating process. The sample is then brushed to remove most of the excess TiO₂ that precipitates on the surface of the crystal instead of in the pores. This improves the homogeneity of the sample for future optical studies.

Formation of the Polymer Support: Due to the fragility of these samples, a thin polymer support is applied to the face of the crystal. This allows the silica spheres to be etched away and the remaining oxide structure to be removed from the quartz slide intact. Poly(allylmethacrylate) (PAMA) is chosen due to its clarity and ease of polymerization. The sintered silica sphere/oxide coating structure is covered by a glass slide of the same dimension with 0.2 mm spacers between them. A prepolymer solution of allyl methacrylate with 1 wt.-% photoinitiator (2,2-dimethoxy-2-phenyl acetophenone) is prepared. Approximately 2 mL of this prepolymer is poured into a small vial. The end of the quartz slide and cover slide are immersed vertically into this prepolymer and capillary forces draw the liquid into the gap between them. This prepolymer is then polymerized with a UV lamp for 6 h, after which the microscope slides are fractured below the filled colloidal crystal and removed from the vial.

Formation of Macropores: The resulting solid structure is immersed in ~10 % aqueous HF solution. The HF solution can penetrate the silica sphere/oxide coating structure through the edges and etch away all silica. The structure is removed and rinsed with water often to remove any etched silica debris from the crystal edges. After a few hours the glass slide and the quartz slide can be removed and the remaining polymer backed macroporous oxide is left in the

solution for several hours to ensure the etching process is complete. Energy dispersive X-ray analysis (EDX) revealed the samples contained <0.2 % Si. The macroporous oxide is then removed from the HF solution and rinsed several times with ultra-pure water from a (18.2 MΩ cm⁻¹) Milli-Q water system and air-dried.

Characterization of Macroporous Oxide Films: The resulting transparent iridescent film is analyzed for homogeneity and pore size using an SEM (Philips XL30 SEM/FEG). The optical properties of these macroporous oxides are evaluated by measuring their transmission spectra at normal incidence using an Ocean Optics ST2000 fiber optic UV–near-IR spectrometer with a 2 mm spot size or a GBC UV-vis 918. X-ray diffraction data was obtained using a Siemens Kristalloflex 710 Diffraktometer.

Received: June 13, 2000
Final version: September 21, 2000

- [1] E. Yablonovitch, *J. Opt. Soc. Am. B* **1993**, *10*, 283.
- [2] S. John, *Phys. Rev. Lett.* **1987**, *58*, 2486.
- [3] K. Busch, S. John, *Phys. Rev. E* **1998**, *58*, 3896.
- [4] M. Megens, J. E. G. J. Wijnhoven, A. Lagendijk, W. L. Vos, *Phys. Rev. A* **1999**, *59*, 4727.
- [5] S.-Y. Lin, E. Chow, V. Hietala, P. R. Villeneuve, J. D. Joannopoulos, *Science* **1998**, *282*, 274.
- [6] O. D. Velev, T. A. Jede, R. F. Lobo, A. M. Lenhoff, *Nature* **1997**, *389*, 447.
- [7] P. Jiang, K. S. Hwang, D. M. Mittleman, J. F. Bertone, V. L. Colvin, *J. Am. Chem. Soc.* **1999**, *121*, 11 630.
- [8] S. H. Park, Y. Xia, *Adv. Mater.* **1998**, *10*, 1045.
- [9] C. G. Göltner, *Angew. Chem. Int. Ed.* **1999**, *38*, 3155.
- [10] S. A. Johnson, P. J. Olliver, T. E. Mallouk, *Science* **1999**, *283*, 963.
- [11] J. E. G. J. Wijnhoven, W. L. Vos, *Science* **1998**, *281*, 802.
- [12] B. Gates, Y. Yin, Y. Xia, *Chem. Mater.* **1999**, *11*, 2827.
- [13] Y. A. Vlasov, N. Yao, D. J. Norris, *Adv. Mater.* **1999**, *11*, 165.
- [14] F. J. P. Schuurmans, D. Vanmaekelbergh, J. van de Lagemaat, A. Lagendijk, *Science* **1999**, *284*, 141.
- [15] P. V. Braun, P. Wiltzius, *Nature* **1999**, *402*, 603.
- [16] H. Yan, C. F. Blanford, B. T. Holland, M. Parent, W. H. Smyrl, A. Stein, *Adv. Mater.* **1999**, *11*, 1003.
- [17] O. D. Velev, P. M. Tessier, A. M. Lenhoff, E. W. Kaler, *Nature* **1999**, *401*, 548.
- [18] P. Jiang, J. Cizeron, J. F. Bertone, V. L. Colvin, *J. Am. Chem. Soc.* **1999**, *121*, 7957.
- [19] B. T. Holland, C. F. Blanford, A. Stein, *Science* **1998**, *281*, 538.
- [20] A. Richel, N. P. Johnson, D. W. McComb, *Appl. Phys. Lett.* **2000**, *76*, 1816.
- [21] G. Subramania, K. Constant, R. Biswas, M. M. Sigalas, K. M. Ho, *Appl. Phys. Lett.* **1999**, *74*, 3933.
- [22] G. Subramanian, V. N. Manoharan, J. D. Thorne, D. J. Pine, *Adv. Mater.* **1999**, *11*, 1261.
- [23] M. S. Thijssen, R. Sprik, J. E. G. J. Wijnhoven, M. Megens, T. Narayanan, A. Lagendijk, W. L. Vos, *Phys. Rev. Lett.* **1999**, *83*, 2730.
- [24] P. Jiang, J. F. Bertone, K. S. Hwang, V. L. Colvin, *Chem. Mater.* **1999**, *11*, 2132.
- [25] A. Hanprasopwattana, S. Srinivasan, A. G. Sault, A. K. Datye, *Langmuir* **1996**, *12*, 3173.
- [26] I. M. Thomas, *Appl. Opt.* **1987**, *26*, 4688.
- [27] C. R. Otterman, K. Bange, *Thin Solid Films* **1996**, *286*, 32.
- [28] H. Hahn, J. Logas, R. S. Averback, *J. Mater. Res.* **1990**, *5*, 609.
- [29] C. J. Brinker, G. W. Scherer, *Sol–Gel Science: The Physics and Chemistry of Sol–Gel Processing*, Academic, San Diego, CA **1990**.
- [30] H. Miguez, F. Meseguer, C. Lopez, A. Blanco, J. S. Moya, J. Requena, A. Mifsud, V. Fornes, *Adv. Mater.* **1998**, *10*, 480.
- [31] R. C. Weast, *CRC Handbook of Chemistry and Physics*, Vol. 66, CRC Press, Boca Raton, FL **1985–86**.
- [32] K.-N. P. Kumar, K. Kelzer, A. J. Burggraaf, *J. Mater. Chem.* **1993**, *3*, 1141.
- [33] A. W. Czanderna, C. N. R. Rao, J. M. Honig, *Trans. Faraday Soc.* **1958**, *54*, 1069.
- [34] H. Zhang, J. F. Banfield, *J. Mater. Res.* **2000**, *15*, 437.
- [35] D. M. Mittleman, J. F. Bertone, P. Jiang, K. S. Hwang, V. L. Colvin, *J. Chem. Phys.* **1999**, *111*, 345.
- [36] J. F. Bertone, P. Jiang, K. S. Hwang, D. M. Mittleman, V. L. Colvin, *Phys. Rev. Lett.* **1999**, *83*, 300.
- [37] The refractive index of the TiO₂ was estimated by fitting the measured transmission spectrum to that predicted by a one-dimensional scalar wave calculation. Pore sizes were fixed by microscopy and the effective index of the material was extracted. Though approximate, this simple model captures many of the semi-quantitative features of the optical spectra along high symmetry axes. See [35].
- [38] W. Stober, A. Fink, E. Bohn, *J. Colloid Interface Sci.* **1968**, *26*, 62.